Int. J. Heat Mass Transfer. Vol. 35, No. 5, pp. 1115–1123, 1992
Printed in Great Britain

0017-9310/92 $5.00+0.00
© 1992 Pergamon Press Ltd

A prediction model of subcooled water flow boiling CHF for pressure in the range 0.1–20 MPa

Y. KATTO

Department of Mechanical Engineering, Nihon University, Kanda-Surugadai, Chiyoda-ku, Tokyo 101, Japan

(*Received* 18 *March* 1991)

Abstract—Existing data for the critical heat flux (CHF) of subcooled water flow boiling have so far been limited within a comparatively high pressure regime, say, from 2.5 to 20.0 MPa. However, under the necessity of high flux removal of heat from fusion reactor components, some experiments have recently been made under low pressures, providing a tolerable number of reliable data for 0.1–2.5 MPa. Corresponding to this situation, this paper reports the result of an attempt of extending the applicable range of the author's previously presented model of subcooled flow boiling CHF to the low pressure regime. The extension is made preserving the structure of the model, and the model is endowed with the capability to predict CHF with nearly the same accuracy over a wide pressure range of 0.1–20.0 MPa.

1. INTRODUCTION

MANY EXPERIMENTAL studies have been made on critical heat flux (CHF) of subcooled water flow boiling in round tubes, so a number of experimental data are available (refs. [1, 2], for example). However, since the foregoing studies are mostly related to the conditions of devices such as nuclear power plants, the existing data with subcooling at the tube exit are in a range of pressures of, say, 2.5–20.0 MPa (corresponding vapor/liquid density ratio $\rho_v/\rho_L = 0.015$–0.35). Several experimental CHF data for nonaqueous fluids are also available (R-11 [3], R-12 [4], nitrogen [5] and helium [6], for example), and it is of interest to note that they are in nearly the same range of vapor/liquid density ratio as that of water.

As for the CHF of subcooled water flow boiling at pressures lower than the above, reliable data with subcooling at the tube exit have so far been scarce. However, under the necessity of high flux removal of heat from fusion reactor components, some experimental studies of CHF have recently been made under conditions of low pressure, high mass velocity, and comparatively small tube diameter [7–9]. These papers provide us with a considerable amount of CHF data (see Table 1 for the range of their experimental conditions).

Now, according to the analyses made in these recent studies, existing CHF correlations or models for subcooled flow boiling seem to lack the capability of giving an accurate prediction of the CHF in the low pressure range. For example, Inasaka and Nariai [8] compared their own CHF data with the modified Tong correlation (which will be explained later), the Weisman–Pei model [10], and the Gunther correlation [11], suggesting the superiority of the modified Tong correlation in prediction accuracy at pressures lower than 1 MPa. The foregoing modified Tong correlation is a correlation proposed by Inasaka and Nariai [12], which has the same form as that of the original Tong correlation [13] for water in the range of 7–14 MPa:

$$q_c/H_{fg} = C \cdot G^{0.4}\mu_L^{0.6}/d^{0.6} \tag{1}$$

except for the coefficient C on the right-hand side of equation (1); that is, instead of the original coefficient C_{Tong}:

Table 1. Experimental data of CHF of subcooled flow boiling

Fluid	No. of data	Data of $\alpha < 0.7$	d (mm)	P (MPa)	G (kg m^{-2} s^{-1})	$T_{sat}-T_L$ (K)	ρ_v/ρ_L	Ref.
Water	374	315	8	2.9–19.6	500–5000	0–75	0.018–0.321	[1]
Water	270†	270	7.72–11.07	3.4–13.8	350–10 360	1.8–97.6	0.021–0.136	[2]
Water	5	5	3	0.77	4600–40 600	30.0–74.07	0.0045	[7]
Water	29	24	3	0.3–1.1	9300–29 900	25.7–37.1	0.0017–0.0061	[8]
Water	43	33	2.5–5.0	0.1–2.2	2207–33 533	15.6–117.5	0.0006–0.013	[9]
Total	721	647						

† Nine clearly abnormal data points have been omitted from the original data.

NOMENCLATURE

c_{pL} specific heat of liquid at constant pressure
d i.d. of tube
f friction factor for homogeneous flow
G mass velocity
h_{FC} forced convection heat transfer coefficient
H_{fg} latent heat of evaporation
k vapor velocity coefficient
L_B length of vapor blanket
P local pressure at CHF onset point
Pr_L Prandtl number of liquid, $\mu_L c_{pL}/\lambda_L$
q heat flux
q_c critical heat flux
q_B fraction of q for boiling
Re Reynolds number of homogeneous flow, Gd/μ
T_L local liquid temperature
T_{sat} saturation temperature
T_w wall temperature
U_B vapor blanket velocity
U_δ homogeneous flow velocity at distance δ from wall
x true quality
x_e local equilibrium quality
$x_{e,N}$ x_e at the incipience of net vapor generation.

Greek symbols
α void fraction
δ sublayer thickness
λ_L thermal conductivity of liquid
μ viscosity for homogeneous flow
μ_L viscosity of liquid
μ_v viscosity of vapor
ρ density for homogeneous flow
ρ_L density of liquid
ρ_v density of vapor
σ surface tension
τ vapor blanket passage time
τ_w wall shear stress of homogeneous flow.

$$C_{Tong} = 1.76 - 7.433x_e + 12.222x_e^2 \quad (2)$$

the following pressure-modified C is employed:

$$\frac{C}{C_{Tong}} = 1 - \frac{52.3 + 80x_e - 50x_e^2}{60.5 + (10P)^{1.4}}. \quad (3)$$

The original Tong correlation, consisting of equations (1) and (2), has a generalized form (that is, critical boiling number q_c/GH_{fg} is a function of Reynolds number Gd/μ_L and exit equilibrium quality x_e), but equation (3) of the modified Tong correlation is not dimensionless, including P [MPa] on the right-hand side.

Meanwhile, Celata *et al.* [9] compared their own CHF data with the Gunther correlation [11], the Lee–Mudawar model [14], and the Katto model [15], suggesting that the existing models or correlations are generally inadequate as regards prediction accuracy in the low pressure regime.

In fact, if the foregoing CHF data in the low pressure regime are compared with the modified Tong correlation (equations (1)–(3)), we obtain the result of Fig. 1. As far as the data of Inasaka and Nariai [8] are concerned, they are certainly predicted by the correlation within the error of approximately $\pm 25\%$, but if the data of Celata *et al.* are taken into account, it assumes a different aspect.

Similarly, comparison with the same CHF data as above gives the result of Fig. 2 for the reformed Katto model [16], which employs a reformed version of the correlation equation of velocity coefficient in the Katto model [15]. In the present case, it is noticed that the prediction accuracy deteriorates increasingly with decreasing pressure in the pressure region lower than 1.7 MPa.

Now, the reformed Katto model mentioned above is a model that holds for the conditions of $\rho_v/\rho_L > 0.01$ and void fraction $\alpha < 0.7$ (see ref. [16]); the remaining low pressure region of $\rho_v/\rho_L < 0.01$ (corresponding pressure $P < 1.7$ MPa in the case of water) has so far been left untouched. In fact, this situation of the reformed Katto model can be observed in Fig. 2, where the prediction error does not exceed $\pm 25\%$ at pressures higher than 1.7 MPa. Thus, it seems worth attempting a study to extend the applicable range of the reformed Katto model to the remaining region of $\rho_v/\rho_L < 0.01$ with the help of the CHF data of refs. [7–9] at low pressures.

2. EXTENSION OF THE APPLICABLE RANGE OF THE MODEL

2.1. *Velocity coefficient k in the high pressure regime*

The reformed Katto model [16] (see the Appendix for its prediction procedure) postulates CHF to be created by the dryout of a liquid sublayer which is built up between the heated tube wall and a vapor blanket flowing over the tube wall. The initial sublayer thickness δ is evaluated by a generalized equation of δ derived in a previous study of CHF in pool boiling [17], while the local velocity U_δ of the two-phase flow (assumed as homogeneous flow) at the distance δ from the tube wall is estimated by the Karman velocity distribution. Then, the vapor blanket velocity U_B, which determines the axial length L_B and the passage

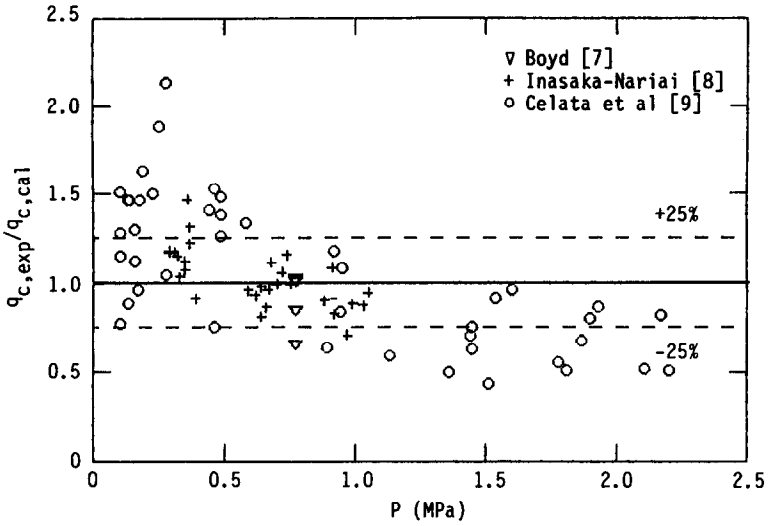

FIG. 1. Comparison between measured and predicted critical heat flux (the modified Tong correlation: the low pressure regime).

time τ of a vapor blanket, is assumed to be closely related to the foregoing local velocity U_δ as:

$$U_B = kU_\delta$$

where the velocity coefficient k on the right-hand side is the only quantity to be determined empirically in this model.

Hence, the magnitude of k can be evaluated for every experimental CHF datum of subcooled flow boiling so that the CHF values predicted by the model may agree with the experimental CHF data; simultaneously, the values of void fraction α and Reynolds number Re are also determined. Then, the values of k thus obtained for the CHF data of refs. [1, 2] were analyzed in a previous paper [16] to reveal that k can be correlated as a function of void fraction α, density ratio ρ_v/ρ_L, and Reynolds number Re as:

$$k = \frac{242[1+K_1(0.355-\alpha)][1+K_2(0.100-\alpha)]}{[0.0197+(\rho_v/\rho_L)^{0.733}][1+90.3(\rho_v/\rho_L)^{3.68}]} Re^{-0.8}. \quad (4)$$

where $K_1 = 0$ for $\alpha > 0.355$, and $K_1 = 3.76$ for $\alpha < 0.355$, while $K_2 = 0$ for $\alpha > 0.1$, and $K_2 = 2.62$ for $\alpha < 0.1$.

In Figs. 3–6, equation (4) is represented by thick lines, while the values of k determined from experimental CHF data are plotted with a symbol ○, for $\alpha = 0$, 0–0.25, 0.25–0.35 and 0.35–0.70, respectively. It is noticed in these figures that equation (4) predicts

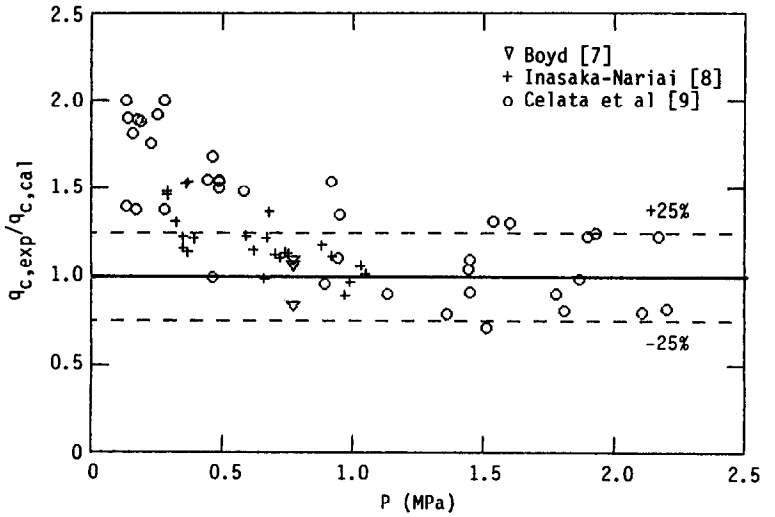

FIG. 2. Comparison between measured and predicted critical heat flux (the reformed Katto model: the low pressure regime).

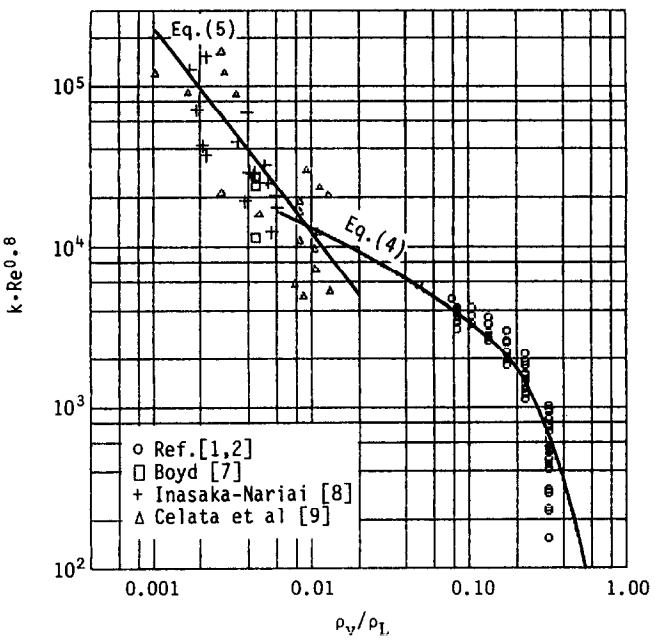

FIG. 3. Velocity coefficient k (void fraction : $\alpha = 0$).

k-values fairly well in the high pressure regime of $\rho_v/\rho_L > 0.01$.

For reference, the ranges of magnitudes of the initial sublayer thickness δ, the vapor blanket length L_B, the vapor blanket velocity U_B, the average velocity in the tube $U\ (=G/\rho)$, and Reynolds number Re, which are determined simultaneously with the evaluation of k, are listed on the upper two lines in Table 2.

2.2. *Velocity coefficient k in the low pressure regime*

The same evaluation of k as that in the preceding section can be made for the CHF data points of water at low pressures obtained by Boyd [7], Inasaka and Nariai [8], and Celata *et al.* [9]. The values of k thus obtained are then plotted in Figs. 3–6 with the symbols □, +, and Δ, respectively. The ranges of magnitudes of the initial sublayer thickness δ, the vapor blanket

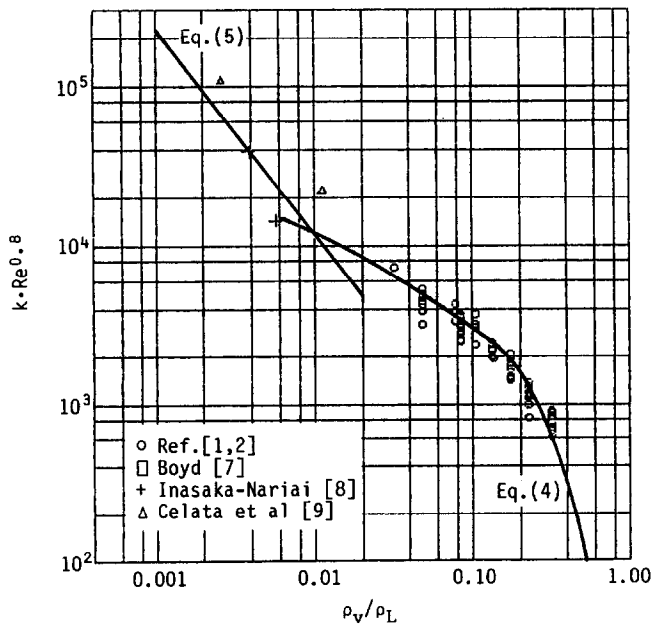

FIG. 4. Velocity coefficient k (void fraction : $0 < \alpha < 0.05$).

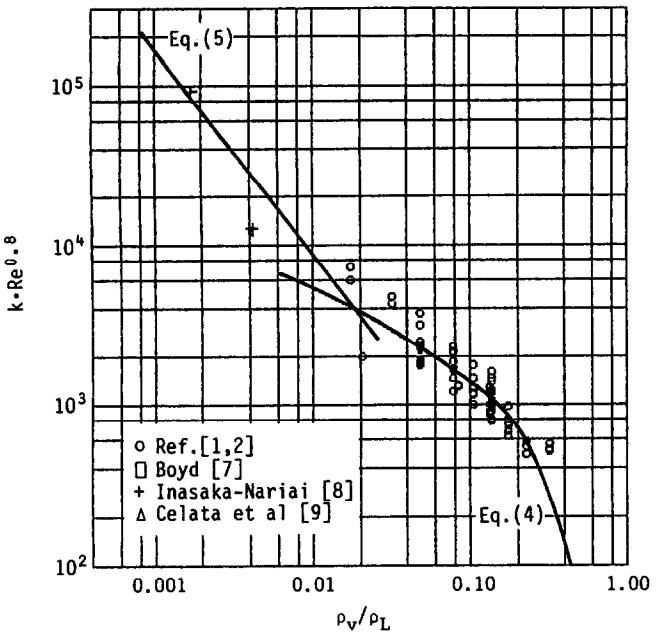

FIG. 5. Velocity coefficient k (void fraction: $0.25 < \alpha < 0.35$).

length L_B, the vapor blanket velocity U_B, the average velocity in the tube U, and Reynolds number Re are also shown on the lower three lines of Table 2; Table 3 is a reclassification of all the data of Table 2 by pressure. According to Tables 2 and 3, it seems likely that there is a rough trend of the initial sublayer thickness δ to be thinner as the pressure is reduced (note that experimental conditions are uncqual for every subdivided region of pressure).

It is noticed in Figs. 3–6 that the data of k in the low pressure regime are limited in number, and scattering is rather high. However, one can see a rough trend that the data in the low pressure regime are located so that they may be connected rather naturally with the data in the high pressure regime. Hence, we assume that k in the low pressure regime can be correlated in a similar form to equation (4), that is, as a function of void fraction α, density ratio ρ_v/ρ_L, and

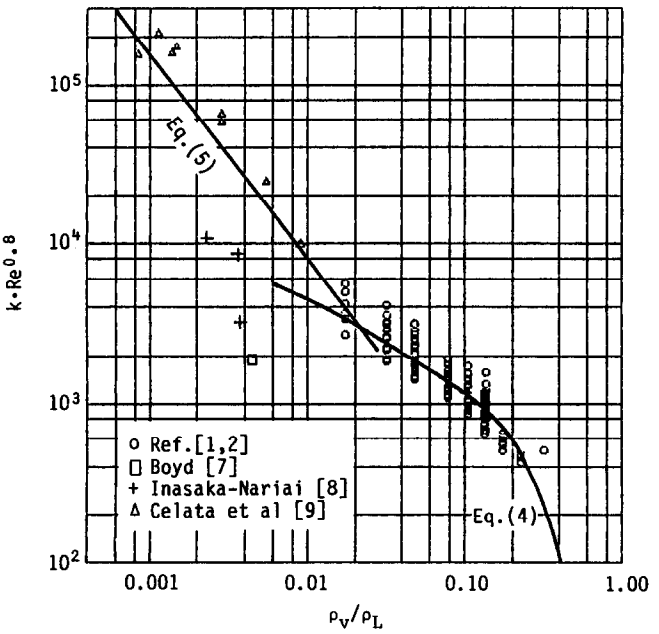

FIG. 6. Velocity coefficient k (void fraction: $0.35 < \alpha < 0.70$).

Table 2. Magnitude of δ, L_B, U_B, U, and Re for the data of $\alpha < 0.7$

Ref.	δ (μm)	L_B (mm)	U_B (m s^{-1})	U (m s^{-1})	Re
[1]	24.3–777.2	1.41–18.2	0.08–1.6	0.84–10.2	4.26×10^4–6.97×10^5
[2]	60.6–493.1	3.64–36.1	0.15–0.8	0.70–14.5	5.09×10^4–1.26×10^6
[7]	1.6–29.5	0.70–17.7	1.99–10.0	4.91–45.2	7.77×10^4–7.61×10^5
[8]	0.5–13.2	0.45–9.3	3.06–18.2	5.78–33.1	9.21×10^4–5.42×10^5
[9]	0.2–23.1	0.35–6.4	1.99–26.4	5.10–36.6	7.28×10^4–5.16×10^5

Table 3. Magnitude of δ, L_B, U_B, U, and Re for the data of $\alpha < 0.7$

P (MPa)	δ (μm)	L_B (mm)	U_B (m s^{-1})	U (m s^{-1})	Re
0.0–2.5	0.2–29.5	0.35–17.7	1.99–26.4	4.91–45.2	7.28×10^4–7.61×10^5
2.5–5.0	24.3–200.2	5.01–36.1	0.54–1.6	2.68–12.2	1.42×10^5–7.56×10^5
5.0–7.5	53.6–230.7	4.50–21.7	0.39–0.9	2.15–14.0	1.13×10^5–1.15×10^6
7.5–10.0	54.9–175.4	3.11–12.9	0.34–0.7	1.23–7.5	6.83×10^4–4.87×10^5
10.0–12.5	55.2–239.1	2.44–15.7	0.26–0.6	0.84–14.5	4.26×10^4–1.26×10^6
12.5–15.0	56.1–493.1	1.95–23.3	0.15–0.5	0.70–8.3	4.26×10^4–5.53×10^5
15.0–17.5	60.3–453.0	1.57–18.2	0.13–0.5	0.89–8.8	4.42×10^4–5.91×10^5
17.5–20.0	80.0–777.2	1.41–16.2	0.08–0.3	0.91–10.2	4.68×10^4–6.97×10^5

Reynolds number Re; a simple correlation equation is determined in the present study as follows:

$$k = 22.4[1+K_3(0.355-\alpha)]/(\rho_v/\rho_L)^{1.28}\,Re^{-0.8} \quad (5)$$

where $K_3 = 0$ for $\alpha > 0.355$, and $K_3 = 1.33$ for $\alpha < 0.355$. Equation (5) is represented by straight lines in Figs. 3–6.

2.3. *Connection of k between the high and low pressure regimes*

We now have two correlation equations (4) and (5) for k, and there is an intersecting point of the two equations in the vicinity of $\rho_v/\rho_L = 0.01$ (see Figs. 3–6). From the physical point of view, there must be a continuous transition region between the two regimes, but because of the scarcity of data, it is difficult to formulate the transition region at the present stage.

Accordingly, it is realistic for the time being to employ equations (4) and (5), neglecting the transition region, to predict the value of k, when the following rule holds for the choice of a proper equation to be adopted under given conditions of α and ρ_v/ρ_L:

equation (4) is used if $\rho_v/\rho_L > (\rho_v/\rho_L)_B$; while

equation (5) is used if $\rho_v/\rho_L < (\rho_v/\rho_L)_B$

where $(\rho_v/\rho_L)_B$ is the value of ρ_v/ρ_L at the intersecting point of the two equations, that is, a root ρ_v/ρ_L of the following equation which is derived by eliminating k from equations (4) and (5):

$$0.09256\frac{[0.0197+(\rho_v/\rho_L)^{0.733}][1+90.3(\rho_v/\rho_L)^{3.68}]}{(\rho_v/\rho_L)^{1.28}} = \frac{[1+K_1(0.355-\alpha)][1+K_2(0.100-\alpha)]}{[1+K_3(0.355-\alpha)]}. \quad (6)$$

The left-hand side of equation (6) is a function decreasing with ρ_v/ρ_L in the vicinity of $\rho_v/\rho_L = 0.01$, so it is quite easy to calculate the value of $(\rho_v/\rho_L)_B$ by computer for a given value of α.

Table 4. Value of $(\rho_v/\rho_L)_B$ at the intersecting point of equations (4) and (5)

α	$(\rho_v/\rho_L)_B$
0.000	0.00885
0.050	0.01060
0.100	0.01307
0.150	0.01394
0.200	0.01504
0.250	0.01648
0.300	0.01844
0.350	0.02128
0.355	0.02164†

† Note: $(\rho_v/\rho_L)_B = 0.02164$ for $\alpha \geqslant 0.355$.

Now, an outline of the values of $(\rho_v/\rho_L)_B$ is shown in Table 4 with a note that $(\rho_v/\rho_L)_B$ is kept at a constant value of 0.02164 for $\alpha \geqslant 0.355$. In other words, $(\rho_v/\rho_L)_B$ takes values between 0.00885 and 0.02164, and hence the following supplementary rule holds: if $\rho_v/\rho_L < 0.00885$, equation (5) plays a dominant role, while if $\rho_v/\rho_L > 0.02164$, equation (4) plays a dominant role.

3. PREDICTION ACCURACY OF THE EXTENDED MODEL

The preceding section has revealed that the applicable range of the reformed Katto model can be extended by an enlargement of the correlation equation of velocity coefficient k to the low pressure regime without any change of the framework of the model. The prediction of CHF value by the extended model then gives the result of Fig. 7 for $\alpha < 0.7$, showing remarkable improvement of the prediction accuracy as compared with Fig. 2.

Finally, if the foregoing extended model is tested

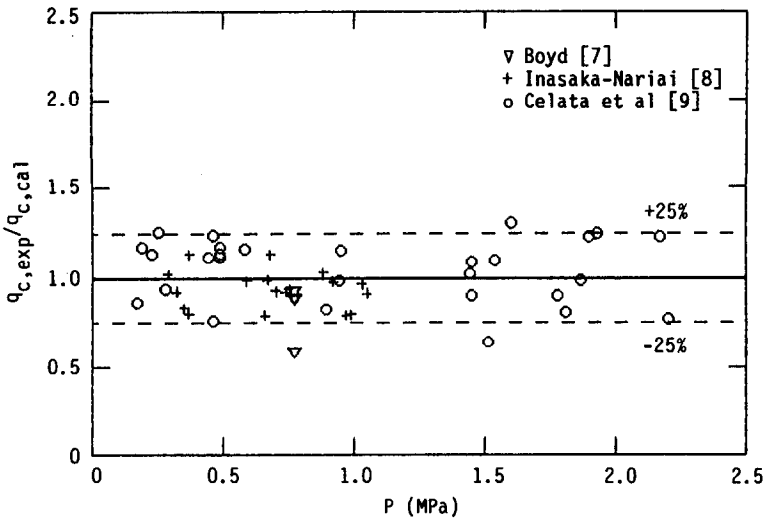

FIG. 7. Comparison between measured and predicted critical heat flux (the extended model: the low pressure regime).

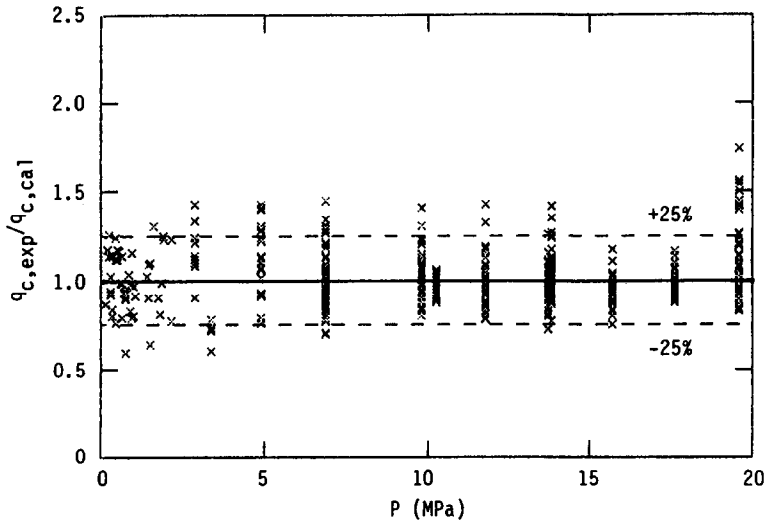

FIG. 8. Comparison between measured and predicted critical heat flux (the extended model: the whole pressure region).

against the whole CHF data points of water listed in Table 1, it gives the result of Fig. 8, where 92.4% of the total of 634 data points for $\alpha < 0.7$ are within the error of $\pm 25\%$. Meanwhile, Table 5 is concerned with the same data points as those in Fig. 8, being reclassified by pressure, where

$$R = q_{c,cal}/q_{c,exp}$$

and $\mu(R)$ is the mean value of R, while $\sigma(R)$ is the standard deviation of R. In Table 5 the number of experimental data points and that of the data points satisfying the condition $\alpha < 0.07$ are also shown. The reason why the total number 634 of the data of $\alpha < 0.7$

Table 5. Prediction accuracy for water CHF

P (MPa)	No. of data	Data of $\alpha < 0.7$	μ (R)	σ (R)
0.0–2.5	77	50	1.0410	0.1916
2.5–5.0	74	36	0.9999	0.2492
5.0–7.5	140	129	1.0493	0.1186
7.5–10.0	43	36	0.9918	0.1308
10.0–12.5	123	120	1.0282	0.0914
12.5–15.0	129	128	1.0216	0.1011
15.0–17.5	45	45	1.0684	0.0888
17.5–20.0	90	90	0.9726	0.1442
Total	721	634	1.0234	0.1348

in Table 5 differs a little from the corresponding number of 647 in Table 1 is as follows: the former number relates to $\alpha < 0.7$ determined in the CHF prediction process by the extended model, while the latter relates to $\alpha < 0.7$ determined in the estimation of k based on the experimental CHF data.

Anyhow, it is noticed from Fig. 8 and Table 5 that the extended model is capable of predicting CHF of subcooled water flow boiling with nearly the same accuracy for pressure in the range 0.1–20.0 MPa; this result is quite interesting when one considers the rather simple theoretical framework of the present model as summarized in the Appendix.

4. CONCLUSIONS

(1) A study has been attempted to extend the applicable range of the author's previously presented model of subcooled flow boiling CHF to the low pressure regime of $\rho_v/\rho_L = 0.0062$–0.01.

(2) Based on the experimental data of CHF of water in the low pressure regime obtained by Boyd, Inasaka–Nariai, and Celata *et al.*, it is revealed that the value of the velocity coefficient k in the low pressure regime has a character to connect naturally with that in the high pressure regime. Hence, by means of extending the correlation equation of k up to the low pressure regime, the foregoing model is endowed with the capability to predict CHF of subcooled water flow boiling with tolerable accuracy over a wide pressure range of 0.1–20.0 MPa.

(3) CHF of water alone is dealt with in the present study. However, according to a previous study [16], the present model is also applicable to the CHF of nonaqueous fluids in the high pressure regime. Hence, it is natural to expect that this situation may possibly remain in the low pressure regime, but strictly speaking, it is a mere supposition until verified by the experimental CHF data of nonaqueous fluids.

REFERENCES

1. Heat Mass Transfer Section, Scientific Council, Academy of Sciences, U.S.S.R., Tabular data for calculating burnout when boiling water in uniformly heated round tubes, *Thermal Engng* **23**(9), 77–79 (1972).
2. B. Thompson and R. V. Macbeth, Boiling water heat transfer burnout in uniformly heated round tubes: a compilation of world data with accurate correlations, U.K.A.E.A., AEEW-R 359 (1964).
3. J. C. Purcupile, L. S. Tong and S. W. Grouse, Jr., Refrigerant–water scaling of critical heat flux in round tubes–subcooled forced-convection boiling, *Trans. ASME*, Ser. C, *J. Heat Transfer* **95**, 279–281 (1973).
4. Y. Katto and S. Yokoya, CHF of forced convection boiling in uniformly heated vertical tubes: experimental study of HP-regime by the use of refrigerant 12, *Int. J. Multiphase Flow* **8**, 165–181 (1982).
5. S. S. Papell, R. J. Simoneau and D. D. Brown, Buoyancy effects on critical heat flux of forced convection boiling in vertical flow, NASA, TN D-3672 (1966).
6. Y. Katto and S. Yokoya, Critical heat flux of liquid helium (I) in forced convection boiling, *Int. J. Multiphase Flow* **10**, 401–413 (1984).
7. R. D. Boyd, Subcooled water flow boiling experiments under uniform high heat flux conditions, *Fusion Technol.* **13**, 131–142 (1988).
8. F. Inasaka and H. Nariai, Critical heat flux of subcooled flow boiling with water, *Proc. NURETH-4*, Karlsruhe, 10–13 October, Vol. 1, pp. 115–120 (1989).
9. G. P. Celata, M. Cumo, G. E. Farello and A. Mariani, Subcooled water flow boiling CHF with very high fluxes, *Revue Gen. Thermique* (1991).
10. J. Weisman and B. S. Pei, Prediction of critical heat flux in flow boiling at low qualities, *Int. J. Heat Mass Transfer* **26**, 1463–1477 (1983).
11. F. C. Gunther, Photographic study of surface-boiling heat transfer to water with forced convection, *Trans. ASME* **73**(2), 115–123 (1951).
12. F. Inasaka and H. Nariai, Critical heat flux and flow characteristics of subcooled flow boiling in narrow tubes, *JSME Int. J.* **30**(268), 1595–1600 (1987).
13. L. S. Tong, Boundary-layer analysis of the flow boiling crisis, *Int. J. Heat Mass Transfer* **11**, 1208–1211 (1968).
14. C. H. Lee and I. Mudawar, A mechanistic critical heat flux model for subcooled flow boiling based on local bulk flow conditions, *Int. J. Multiphase Flow* **14**, 711–728 (1988).
15. Y. Katto, A physical approach to critical heat flux of subcooled flow boiling in round tubes, *Int. J. Heat Mass Transfer* **33**, 611–620 (1990).
16. Y. Katto, Prediction of critical heat flux of subcooled flow boiling in round tubes, *Int. J. Heat Mass Transfer* **33**, 1921–1928 (1990).
17. Y. Haramura and Y. Katto, A new hydrodynamic model of critical heat flux, applicable widely to both pool and forced convection boiling on submerged bodies in saturated liquids, *Int. J. Heat Mass Transfer* **26**, 389–399 (1983).

APPENDIX. CHF PREDICTION PROCEDURE

Assume a value of q under local bulk conditions of P, G, $T_{sat}-T_L$, and d.

Necessary physical properties are (saturated state at P): c_{pL}, H_{fg}, λ_L, μ_L (or ν_L), μ_v (or ν_v), ρ_L, ρ_v and σ.

Calculation of δ:

$$\frac{\delta\rho_v}{\sigma}\Big/\left(\frac{\rho_v H_{fg}}{q_B}\right)^2 = \frac{\pi(0.0584)^2}{2}\left(\frac{\rho_v}{\rho_L}\right)^{0.4}\left(1+\frac{\rho_v}{\rho_L}\right)$$

where $q_B = q - h_{FC}(T_w - T_L)$, for which

$$h_{FC} = 0.023(Gd/\mu_L)^{0.8}\,Pr_L^{0.4}(\lambda_L/d)$$

$$T_w - T_L = \frac{(\Psi_0 - 1)(T_{sat}-T_L)+(q/h_{FC})}{\Psi_0}$$

$$\Psi_0 = 230(q/GH_{fg})^{0.5}.$$

Calculation of x_e and $x_{e,N}$:

$$x_e = \frac{c_{pL}(T_L - T_{sat})}{H_{fg}}$$

$$x_{e,N} = \begin{cases} -0.0022\dfrac{q}{\rho_L H_{fg}}\dfrac{d}{(\lambda_L/c_{pL}\rho_L)} & \text{for } \dfrac{Gc_{pL}d}{\lambda_L} < 70\,000 \\ -154\dfrac{q}{\rho_L H_{fg}}\dfrac{1}{(G/\rho_L)} & \text{for } \dfrac{Gc_{pL}d}{\lambda_L} > 70\,000. \end{cases}$$

Calculation of x:

$$x = \begin{cases} \dfrac{x_e - x_{e,N}\exp\left(\dfrac{x_e}{x_{e,N}} - 1\right)}{1 - x_{e,N}\exp\left(\dfrac{x_e}{x_{e,N}} - 1\right)} & \text{for } x_{e,N} < x_e \\ 0 & \text{for } x_{e,N} > x_e. \end{cases}$$

Calculation of ρ, α, and μ:

$$\rho = 1/[x/\rho_v + (1-x)/\rho_L]$$
$$\alpha = x/[x + (1-x)(\rho_v/\rho_L)]$$
$$\mu = \mu_v\alpha + \mu_L(1-\alpha)(1+2.5\alpha).$$

Calculation of U_δ:

$$U_\delta^+ = \begin{cases} y_\delta^+ & \text{for } 0 < y_\delta^+ < 5 \\ 5.0 + 5.0 \ln (y_\delta^+/5) & \text{for } 5 < y_\delta^+ < 30 \\ 5.5 + 2.5 \ln y_\delta^+ & \text{for } 30 < y_\delta^+ \end{cases}$$

where $U_\delta^+ = U_\delta/\sqrt{(\tau_w/\rho)}$ and $y_\delta^+ = \delta\sqrt{(\tau_w/\rho)}/(\mu/\rho)$ for which

$$\tau_w = f \cdot \rho(G/\rho)^2/8$$
$$1/\sqrt{f} = 2.0 \log_{10} (Re\sqrt{f}) - 0.8$$
$$Re = Gd/\mu.$$

Calculation of k:

k: equation (4) for $\rho_v/\rho_L > (\rho_v/\rho_L)_B$

k: equation (5) for $\rho_v/\rho_L < (\rho_v/\rho_L)_B$

where $(\rho_v/\rho_L)_B$ is a root of equation (6).

Calculation of U_B:

$$U_B = kU_\delta.$$

Calculation of L_B:

$$L_B = 2\pi\sigma(\rho_v + \rho_L)/(\rho_v\rho_L U_B^2).$$

Calculation of q':

$$q' = \delta\rho_L H_{fg}/\tau$$

where $\tau = L_B/U_B$; q is the critical heat flux q_c when $q = q'$.

UN MODELE PREDICTIF DU CHF D'UN ECOULEMENT D'EAU EN EBULLITION POUR DES PRESSIONS DE 0,1–20 MPa

Résumé—Les données existantes sur le flux thermique critique (CHF) d'un écoulement d'eau sous-refroidie portée à ébullition sont limitées à un domaine de pression comparativement élevé, de 2,5 à 20 MPa. Sous la nécessité de l'enlèvement de chaleur à grand flux pour les composants du réacteur de fusion, quelques expériences ont été récemment conduites sous pression faible pour obtenir un nombre significatif de données entre 0,1 et 2,5 MPa. En conséquence, ce texte rapporte le résultat d'un essai pour étendre le domaine d'application d'un modèle présenté antérieurement par l'auteur. L'extension est faite en préservant la structure du modèle lequel est capable de prédire le CHF avec à peu près la même précision dans le domaine de pression 0,1–20 MPa.

EIN MODELL ZUR BESTIMMUNG DER KRITISCHEN WÄRMESTROMDICHTE FÜR UNTERKÜHLTES STRÖMUNGSSIEDEN VON WASSER BEI DRÜCKEN ZWISCHEN 0,1 UND 20 MPa

Zusammenfassung—Die bisher bekannt gewordenen Daten für die kritische Wärmestromdichte bei unterkühltem Strömungssieden von Wasser beschränken sich auf einen Bereich relative hoher Drücke (2,5–20,0 MPa). Kürzlich wurden jedoch einige Experimente bei niedrigen Drücken durchgeführt, die im Zusammenhang mit der Notwendigkeit stehen, aus Bauteilen von Fusionsreaktoren sehr große Wärmestromdichten abzuführen. Sie liefern eine genügende Menge zuverlässiger Daten für Drücke zwischen 0,1 und 2,5 MPa, um den Gültigkeitsbereich des vom Autor an anderer Stelle vorgestellten Modells für die Bestimmung der kritischen Wärmestromdichte beim unterkühlten Strömungssieden zu niedrigeren Drücken hin zu erweitern. Dabei bleibt die Struktur des Modells unverändert. Es erlaubt die Bestimmung der kritischen Wärmestromdichte mit nahezu gleichbleibender Genauigkeit in dem weiten Druckbereich von 0,1–20,0 MPa.

РАСЧЕТНАЯ МОДЕЛЬ КРИТИЧЕСКОГО ТЕПЛОВОГО ПОТОКА ПРИ ТЕЧЕНИИ КИПЯЩЕЙ НЕДОГРЕТОЙ ВОДЫ В ДИАПАЗОНЕ ДАВЛЕНИЙ ОТ 0,1 ДО 20 MPa

Аннотация—Имевшиеся данные по критическому тепловому потоку при течении кипящей недогретой воды ограничивались рамками режима с относительно высокими давлениями: от 2,5 до 20,0 MPa. Однако для решения проблемы отвода теплового потока большой плотности от компонентов термоядерного реактора в последнее время было проведено несколько экспериментов при низких давлениях, которые дали довольно польшое число надежных данных для давлений от 0,1 до 2,5 MPa. В настоящей статье приведены результаты исследований, в которых предпринята распространить диапазон ранее представленной автором модели критического теплового потока при течении кипящей недогретой жидкости на ржим с низким давлением. Это обобщение проведено с сохранением структуры модели. Исследована возможность рассчитать критический тепловой поток почти с такой же точностью в широком диапазоне давлений от 0,1 до 20,0 MPa.